

Mid-spatial frequency errors of mass-produced aspheres

Wilhelmus A. C. M. Messelink^a, Amy Frantz^a, Shelby D. V. Ament^b, and Matthew Stairiker^b

^aEdmund Optics Singapore Pte. Ltd., 18 Woodlands Loop #04-00, Singapore, Singapore

^bEdmund Optics Headquarters, 101 East Gloucester Pike, Barrington, USA

ABSTRACT

For the (CNC) polishing of aspheres, generally a compliant, sub-aperture tool is applied, which may cause mid-spatial frequency errors on the surface of the workpiece. The tolerance on surface figure is commonly given in peak-to-valley (PV) or root-mean-square (RMS). Even if a surface is fabricated within specified tolerances according to one of the mentioned metrics, the optical performance may be inadequate for the desired application. For the specification of the tolerance on mid-spatial frequency errors, several other characteristics have been proposed, e.g. power spectral density (PSD) or surface slope error. This paper presents an investigation into the mid-spatial frequency form error of mass-produced aspheres, discusses the results and draws relevant conclusions.

Keywords: Mid-spatial frequency, Slope error, Asphere

1. INTRODUCTION

Allowable surface form error of aspheres is traditionally specified using figures of merit such as peak-to-valley (PV) and root-mean-square (RMS), which are well-established in the optics industry. In contrast to the PV, which only considers the two extreme points on the lens, the RMS is better correlated to optical performance due to its consideration of all points on the lens. However, neither gives a full picture of how optical system performance will be affected by manufacturing deviations from optical designs. A good example of process-introduced, mid-spatial frequency errors is presented by Aikens et al.¹

One key performance metric for aspheres is Strehl ratio: the ratio of the peak irradiance of the focused spot from the as-built lens compared to the peak focal irradiance of a diffraction limited lens with the same diameter and focal length. Strehl ratio is closely approximated by the following expression:²

$$S = e^{-k^2\sigma^2}$$

where $k=2\pi/\lambda$, λ is wavelength, and σ is RMS wavefront error. While Strehl ratio can be calculated from RMS wavefront error, it cannot be directly linked to a surface measurement without an understanding of the exact nature of the error. For example, two surface form error maps with the same PV or RMS error values but different spatial frequency content will have different impacts on the Strehl ratio, see Figure 1.

Spatial frequency content of an irregularity map can be targeted and controlled in several different ways [3, Chapter 7]. A direct method of analysis is to generate a Power Spectral Density (PSD) plot and set tolerances on this plot.⁴ ISO 10110-8 on roughness and waviness describes how PSD can be toleranced.⁵

However, it is clear that for a given PV form error, higher spatial frequencies have a more detrimental impact on Strehl ratio. One way of limiting higher spatial frequency error is to set a maximum slope or maximum RMS slope for the surface form error map. This specification in combination with a PV form error acts as a low pass filter for spatial frequency content, See Figure 2.

A method of measuring and specifying maximum and RMS surface slope error is described in ISO 10110-5⁶ and ISO10110-14.⁷ Several aspects of the measurement must be defined, such as orientation (radial, tangential, absolute), spatial sampling interval (lateral resolution of the measurement system), and sampling length (window size).

Send correspondence to: Wilhelmus A. C. M. Messelink, E-mail: pmesselink@edmundoptics.com.sg, Telephone: +65 6273 6644

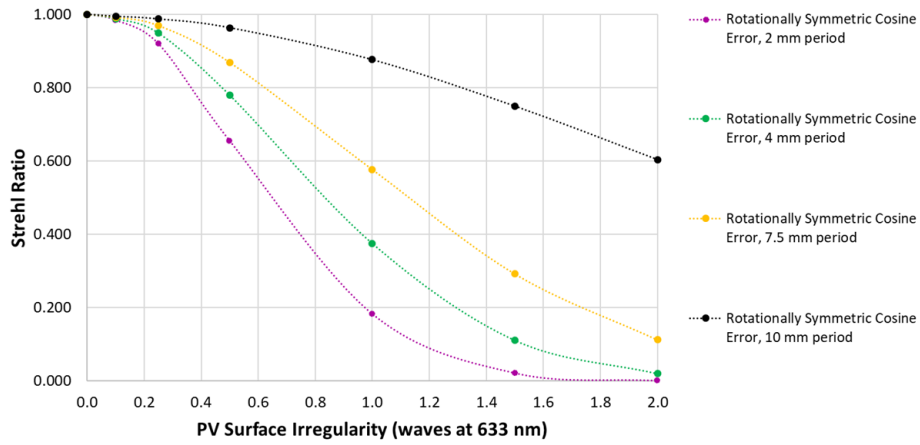


Figure 1. Strehl versus PV Surface Irregularity applied to a 50 mm f/0.6 asphere, showing the effect of spatial frequency content on Strehl Ratio.

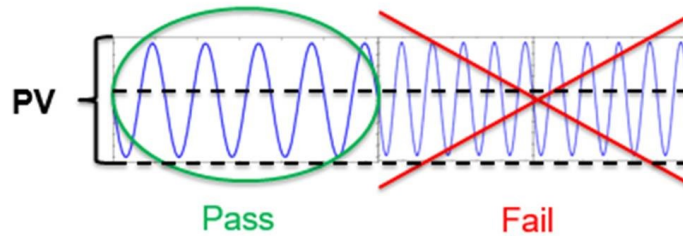


Figure 2. Representation of slope specification in combination with PV surface form error used to limit high spatial frequency content.

Customers are more frequently requesting slope tolerances with a variety of window sizes. Because it is impossible to analyze manufacturing capabilities ahead of time for all possible window sizes that a customer may request, a general relationship that approximates the slope error for a continuous spectrum of window sizes is desired.

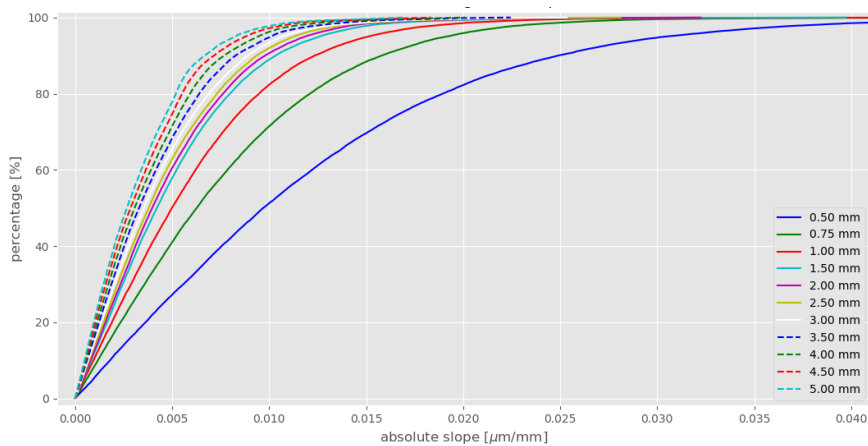


Figure 3. Cumulative distributions of the absolute tangential slope for various window sizes.

Other recent, but more uncommon, customer inquiries have been regarding the tangential slope error as well

as the distribution of the slope error (instead of the maximum or RMS value). As an example, Figure 3 shows the cumulative distributions of a CNC polished surface for different window sizes.

2. METHODOLOGY

2.1 Outline

For this investigation we analyzed the slope error for different window sizes on production aspheres, which underwent standard CNC grinding and CNC sub-aperture polishing. This mass-production environment currently uses peak to valley and RMS errors as a customer target metric for corrective grinding and polishing, and does not regularly quantify slope errors. Therefore, these types of errors have been largely uncontrolled and unexamined.

The lenses were measured using an OptiPro UltraSurf 4X 100 Metrology System, which provides a two-dimensional measurement of the deviation from the nominal aspheric form. Furthermore the measurements were detrended by subtracting power, as per ISO14999-4.⁸ In addition to evaluating the slope error of the two-dimensional measurements, one-dimensional slices through the center of the lens were taken from the same measurements and the (radial) slope error was calculated from those as well.

Various units for slope error are used in the industry, including milliradians, arcminutes, micrometer over the stated window size, and micrometer per millimeter.⁹ For this investigation the unit $\mu\text{m}/\text{mm}$ is used regardless of the window size under test.

Specifically, we analyzed window sizes of 0.5, 0.75, 1.0, 1.5, 2.0, 2.5, 3.0, 3.5, 4.0, 4.5 and 5.0 mm, which we examined for both the maximum and RMS absolute slope error, as well as the position of the maximum absolute slope, which may indicate the root cause of that error.

2.2 Radial and tangential slope error

Because two-dimensional measurement data is generally provided on a regular grid, the slope error for a certain point P is calculated in Cartesian space:

$$\vec{S} = \begin{pmatrix} S_x \\ S_y \end{pmatrix},$$

where S_x equals the slope in the x -direction, and S_y equals the slope in the y -direction.

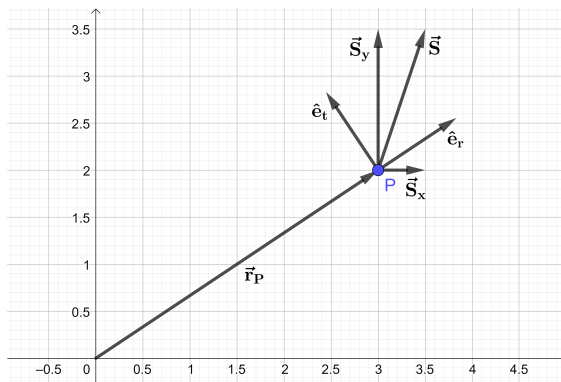


Figure 4. Diagram outlining the conversion from Cartesian to Cylindrical slope.

To change the basis from Cartesian to Cylindrical, first the radial and tangential unit vectors need to be calculated, see Figure 4:

$$\hat{e}_r = \frac{\vec{r}_P}{\|\vec{r}_P\|}, \quad \hat{e}_t = \begin{bmatrix} 0 & -1 \\ 1 & 0 \end{bmatrix} \cdot \hat{e}_r,$$

where \hat{e}_r and \hat{e}_t are the radial and tangential unit vectors respectively and $\vec{r}_P = \begin{pmatrix} P_x \\ P_y \end{pmatrix}$ denotes the position on the surface. The conversion then becomes:

$$S_r = \vec{S} \cdot \hat{e}_r = \frac{S_x P_x + S_y P_y}{\sqrt{P_x^2 + P_y^2}}, \quad (1)$$

$$S_t = \vec{S} \cdot \hat{e}_t = \frac{S_y P_x - S_x P_y}{\sqrt{P_x^2 + P_y^2}}. \quad (2)$$

It follows that the conversion depends on the x - and y -coordinate of measurement data.

2.3 Implementation

Equations 1 and 2 have been implemented in two softwares: the QED.NET Toolkit and the Python program language, which is detailed in the following sections.

2.3.1

The QED.NET Toolkit is part of a suite of software from QED Technologies that supports their family of polishing and metrology platforms. It allows the user to build a graphical program of a sequence of mathematical computations to be performed on imported metrology data (e.g. subtraction of two-dimensional error maps).

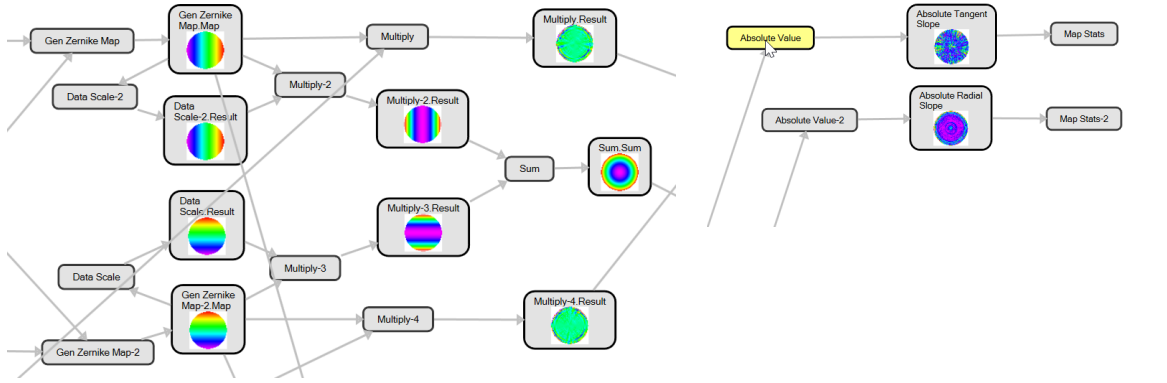


Figure 5. Diagram outlining parts of the graphical program to convert Cartesian to Cylindrical slope in QED.NET Toolkit.

As the software does not provide calculations using the x - and y -coordinate of measurement data, these have been implemented by generating two-dimensional maps using Zernike polynomials, which are supported, namely tip (Z_1^1), for the x -coordinate, and tilt (Z_1^{-1}) for the y -coordinate, as shown in Figure 5. As a sanity check the magnitude of the combined radial and tangential slope error has been compared to the magnitude of the combined slopes in x and y , and the difference was found to be in the order of 10^{-16} , which is in line with floating point rounding errors. This confirms that the QED.NET toolkit, with some programming effort, can be used to analyze radial and tangential slope errors of two-dimensional metrology data.

2.3.2 Python

For the remainder of the study, more flexibility and automation of the analysis was required, and as such, equations 1 and 2 were implemented in the Python computer language. Figure 6 shows screenshots of the implementation, demonstrating the analysis of a single two-dimensional measurement (right) and the analysis of a one-dimensional slice through the center of the same measurement.

As a sanity check, the results were compared to the results from the earlier implementation in QED.NET, and they matched qualitatively as well as provided the same maximum and RMS values.

With this implementation it was possible to analyze multiple metrology files at multiple specified window sizes and collate the results automatically. The maximum and RMS absolute radial slope error were investigated

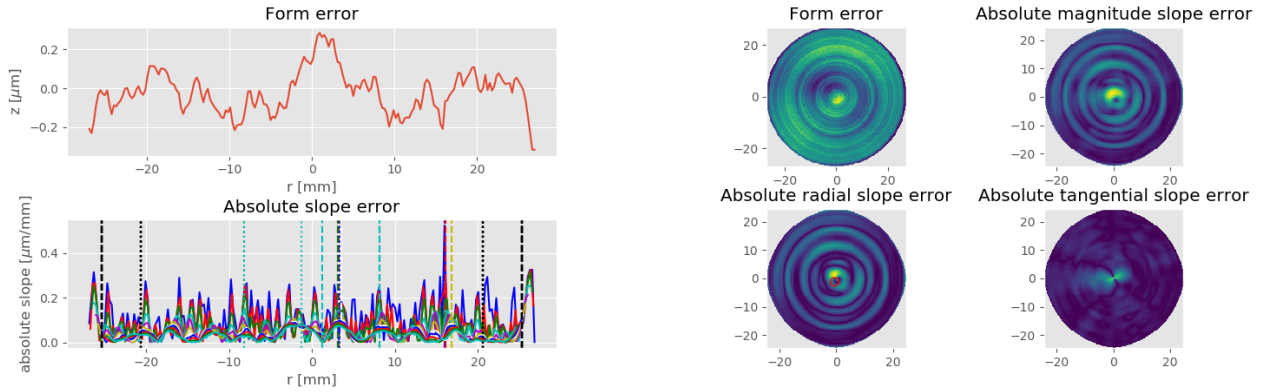


Figure 6. Screenshots of the implementation of the slope analysis in Python.

over the bulk area (defined as the outer diameter of the lens minus the diameter of the tool contact area of the last polishing process used minus the largest window size under investigation) for window sizes between 0.5 and 5.0 mm. Furthermore the location of the maximum absolute radial slope error was investigated for the same window sizes over the full diameter of the available metrology data (measurement diameter minus the largest window size). The next section reports the results of this investigation.

3. RESULTS

A total of 23 aspheric lenses of the same prescription were made available for this investigation. They had undergone the standard mass-production CNC grinding and polishing process. Their specification did not call for any slope error tolerance and as such the manufacturing process had not been optimized for any particular slope error. The lenses were measured using an OptiPro UltraSurf 4X 100 Metrology System, which provides a two-dimensional measurement of the deviation from the nominal aspheric form. Furthermore, the measurements were detrended by subtracting power, as per ISO14999-4.⁸ In addition to evaluating the slope error of the two-dimensional measurements, one-dimensional slices through the center of the lenses were taken from the same measurements and the (radial) slope error was calculated from those as well.

3.1 Maximum versus RMS absolute radial slope error

The maximum slope error of all 23 aspheres in the test has been compared to the RMS slope error for window sizes between 0.5 and 5.0 mm.

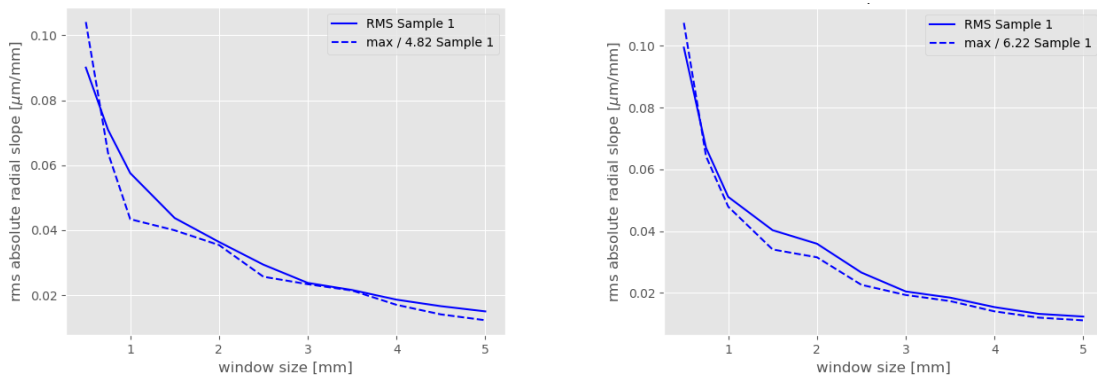


Figure 7. Example plots of the maximum and RMS absolute radial slope error versus window size for a single two-dimensional measurement (right) and a one-dimensional slice through the center (left).

Figure 7 shows an example of the results for one of the aspheric lenses with the two-dimensional measurement on the right and a one-dimensional slice through the center on the left. The plot for the maximum slope error has been divided by a factor, which has been optimized to minimize the difference between the plots of the maximum and the RMS slope error.

Table 1. Results of the fit of the maximum versus RMS absolute radial slope error for window sizes between 0.5 and 5.0 mm

	1-dim	2-dim
Average R^2	0.937	0.954
Mean ratio	4.7	6.2
St. dev. ratio	0.2	0.6

The results of this least squares optimization are summarized in Table 1, which shows that, for both the two- and one-dimensional data, the plots are proportional with a ratio of 6.2 and 4.7 respectively. The average R^2 shows a good fit of the proportional data.

3.2 Maximum slope versus window size

The results from the previous section seem to indicate that there is a hyperbolic trend between the absolute slope error (whether maximum or RMS) and the window size:

$$y = \frac{a}{x - c} + d \quad (3)$$

In general, when a workpiece is measured, tip and tilt are removed from the measurement data, as it is often not possible to differentiate between those introduced by the metrology system and those present on the optic. If tip and tilt are removed from the measurement data then, by definition, the slope error approaches zero when the window size is increased to the clear aperture.

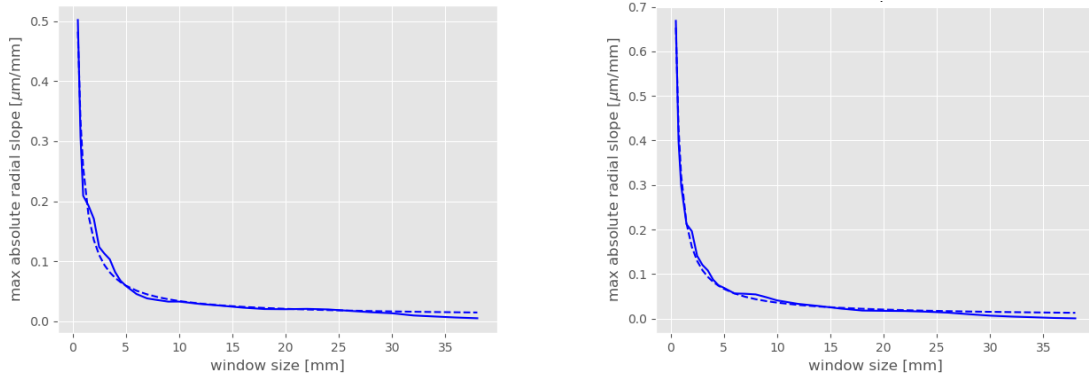


Figure 8. Plot of the maximum absolute radial slope versus window size and a hyperbolic curve fit for a single two-dimensional measurement (right) and a one-dimensional slice through the center (left).

Figure 8 demonstrates how the maximum slope error approaches zero for a typical measurement. As such $d = 0$ in Equation 3. For all 23 measurements, the maximum absolute radial slope error has been analyzed over the bulk area for window sizes between 0.5 and 5.0 mm and parameters a and c of Equation 3 have been least squares fitted to each measurement.

The resulting 23 plots of the maximum slope error versus window size is shown in Figure 9, as well as the fitted hyperbolic curve for each plot.

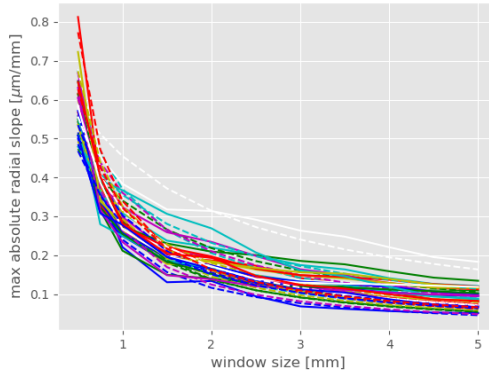


Figure 9. Plots of the maximum absolute radial slope versus window size for 23 measurements and hyperbolic fit.

The results of the hyperbolic fits are summarized in Table 2, of which the minimum and average R^2 show a good fit. The standard deviation of both parameters a and c is on the order of the mean of each parameter, indicating there is no general value for either the a or c parameter and both have to be fitted to each measurement individually to achieve a good fit.

Table 2. Results of the hyperbolic fit of the maximum absolute radial slope error versus window sizes between 0.5 and 5.0 mm.

Quantity	Value	Quantity	Value
Minimum R^2	0.860	Average R^2	0.942
Mean a	0.395	St. dev. a	0.169
Mean c	-0.216	St. dev. c	0.328

3.3 Position of maximum slope

In addition to analyzing the maximum and RMS slope error values, the radial position of the maximum slope has been investigated over the full diameter of the available metrology data. The location of the maximum slope error may indicate the root cause of that error, which facilitates the control of the error. The maximum slope errors are expected to be concentrated at the center of the lens and/or in proximity to the outer diameter. A large slope error at the center of the lens may be due to a misalignment of the tool axis and the part axis during CNC grinding or polishing. Large slope errors near the outer diameter may be caused by the edge-roll effect due to the use of a compliant polishing tool traveling off and returning back onto the lens.

The distance from the center of the optic to the edge has been divided into 10 “buckets” and the position of the maximum slope error of each of the 23 measurements for a given window size has been sorted into one of the buckets, creating a “histogram” of the position of maximum slope error. Figure 10 shows the combined histograms for the window sizes between 0.5 and 5.0 mm. It shows that the majority of maximum slope errors occur near the center of optic or near the edge.

4. CONCLUSIONS

The absolute radial slope error of two-dimensional measurements of 23 mass-produced aspheres, as well as one-dimensional slices through the center of the lens from the same measurements, have been analyzed for window sizes between 0.5 and 5.0 mm.

The relationship between the maximum and RMS slope error has been investigated and it was found that they are proportional, with a ratio of approximately 5.5, analogous to the rule-of-thumb for the ratio between PV and RMS figure error.

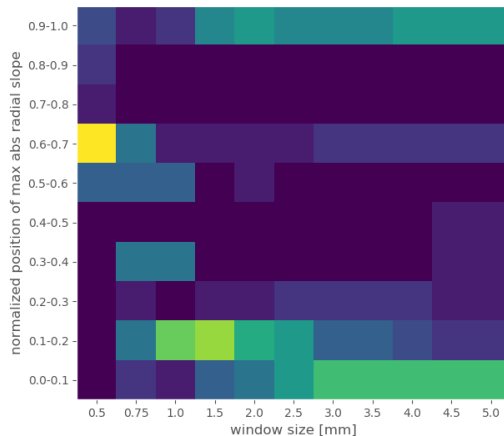


Figure 10. Histogram of the position of the maximum absolute radial slope error for different window sizes for 23 measurements.

The plot of the maximum slope error versus window size follows a hyperbolic curve: $y = \frac{a}{x-c}$, of which the a or c parameter both have to be fitted to each measurement individually to achieve a good fit. Commonly in the optics industry a single window size is used to specify a slope tolerance or to advertise manufacturing capability. It is suggested here that the relationship between maximum slope error for a mass produced asphere is better described by two points along the curve instead of just one.

The position of the maximum absolute radial slope error often lies near the center of the optic or near the edge. A large slope error at the center of the lens may be due to a combination of misalignment of the tool axis and the part axis during CNC grinding or polishing. Large slope errors near the outer diameter may be caused by the edge-roll effect due to the use of a compliant polishing tool traveling off and returning back onto the lens. Therefore it may be beneficial to specify multiple slope tolerances: one for the bulk and one for the edge zone, to reduce manufacturing cost.

REFERENCES

- [1] Aikens, D., DeGroot, J. E., and Youngworth, R. N., “Specification and control of mid-spatial frequency wavefront errors in optical systems,” in [*Frontiers in Optics 2008/Laser Science XXIV/Plasmonics and Metamaterials/Optical Fabrication and Testing*], *Frontiers in Optics 2008/Laser Science XXIV/Plasmonics and Metamaterials/Optical Fabrication and Testing*, OTuA1, Optical Society of America (2008).
- [2] Mahajan, V. N., “Strehl ratio for primary aberrations in terms of their aberration variance,” *J. Opt. Soc. Am.* **73**, 860–861 (Jun 1983).
- [3] Messelink, W. A. C. M., *Numerical methods for the manufacture of optics using sub-aperture tools*, PhD thesis, UCL (University College London) (Oct. 2015).
- [4] Aikens, D. M., Wolfe, C. R., and Lawson, J. K., “Use of power spectral density (psd) functions in specifying optics for the national ignition facility,” in [*International Conference on Optical Fabrication and Testing*], Kasai, T., ed., *Proc. SPIE* **2576**, 281–292, SPIE (1995).
- [5] “Optics and photonics – Preparation of drawings for optical elements and systems – Part 8: Surface texture; roughness and waviness,” standard, International Organization for Standardization, Geneva, CH (Oct. 2010).
- [6] “Optics and photonics – Preparation of drawings for optical elements and systems – Part 5: Surface form tolerances,” standard, International Organization for Standardization, Geneva, CH (Aug. 2015).
- [7] “Optics and photonics – Preparation of drawings for optical elements and systems – Part 14: Wavefront deformation tolerance,” standard, International Organization for Standardization, Geneva, CH (Sept. 2007).
- [8] “Optics and photonics – Interferometric measurement of optical elements and optical systems – Part 4: Interpretation and evaluation of tolerances specified in ISO 10110,” standard, International Organization for Standardization, Geneva, CH (Aug. 2005).

- [9] Kumler, J. J. and Caldwell, J. B., “Measuring surface slope error on precision aspheres,” in [*Optical manufacturing and testing VII*], Burge, J. H., Faehnle, O. W., and Williamson, R., eds., *Proc. SPIE* **6671**, 66710U–66710U–9, SPIE (2007).